JOURNAL OF MATERIALS SCIENCE 30 (1995) 6151–6155

Effect of fluorine content on crystallization of canasite glass-ceramics

S. LIKITVANICHKUL, W. C. LACOURSE
New York State College of Ceramics at Alfred University, Alfred, NY 14802, USA

The effect of fluorine (F) content in the parent glass on nucleation and crystallization of glass-ceramics with canasite as the principle crystalline phase have been studied using differential thermal analysis, X-ray diffraction, and transmission electron and scanning electron microscopies. CaF_2 precipitation occurred during the nucleation phase at all concentrations studied. However, canasite formation during subsequent crystallization was strongly dependent on F content. Canasite failed to form at both high and low concentrations of F, while with intermediate F concentrations canasite and CaF_2 were the only phases identified. Agrellite ($NaCa_2Si_4O_{10}F$) formed when the F content was high.

1. Introduction

Glass-ceramics based on chain silicates, e.g. enstatite ($MgSiO_3$), potassium fluorrichterite ($KNaCaMg_5Si_8O_{22}F_2$) and fluor-canasite ($K_2Na_4Ca_5Si_{12}O_{30}F_4$), which are single, double and multiple chain silicates, respectively, exhibit a combination of high fracture strength and high fracture toughness [1–4]. Canasite glass-ceramics manifest a randomly-oriented interlocking bladed morphology. This random orientation is predetermined by the homogeneous nucleation of CaF_2 crystals in the early stages of the heat treatment process [2]. This lath-like microstructure has a preferred crystallographic cleavage plane and an anisotropic thermal expansion which promotes both crack deflection and anisotropic thermal expansion stress microcracking as toughening mechanisms [1, 2, 4].

Another possible crystalline phase developing from the fluorosilicate glass is agrellite ($NaCa_2Si_4O_{10}F$). Agrellite is also nucleated by CaF_2 to form an interlocking lath-like structure, but glass-ceramics containing this phase have lower fracture strengths (ca. 200 MPa versus ca. 300 MPa for canasite) [1, 5].

Since F is needed both for the formation of nuclei and crystalline phases, the F content in the parent glass plays an important role in controlling the types of crystalline phases formed and the microstructure of canasite glass-ceramics.

2. Experimental procedure

Glasses were prepared from reagent grade CaF_2, $CaCO_3$, SiO_2, Al_2O_3, K_2CO_3 and Na_2CO_3. Compositions of glasses melted here were based on information from Beall's patent [6], provided in Table I. The amount of F was varied while holding the Ca content constant by the amount of CaF_2 and CaO, from 8.6 to 18.6 and 14.6 to 4.6, respectively. Batches were melted for 1 h in covered Pt crucibles in an electric furnace at 1350 °C. Glasses were cast in graphite moulds, were annealed for 30 min at 10 K above their transformation temperatures (as determined by differential scanning calorimetry) and cooled in the furnace.

Glass transition temperatures (T_g) were determined by a differential scanning calorimetry (Mettler DSC30 with Mettler TC111 TA Processor) using a chip of quenched glass weighing 20–25 mg, at a heating rate of 10 K min^{-1}. T_gs were evaluated using the tangent intersection method. Densities were measured in kerosene by Archimedes' technique.

Fluorine contents in the glasses were investigated using a Phillips X-ray fluorescence unit (model PW-1480/10) operating with a Cr–Au alloy X-ray tube at 45 kV and 60 μA. The crystal used as monochromator was a PX1; the detector was a flow-counter analysing the K_α radiation of F atoms.

The thermal behaviour of the glasses was determined by using a Perkin-Elmer DTA with a System 7/4 controller. The glasses were ground to a coarse powder, 30–40 mesh. Runs were made on 50 mg samples in a Pt crucible. The accuracy of the instrument was verified using Ag standards. The measurements were carried out at a heating rate of 10 K min^{-1} with a maximum temperature of 850 °C. The DTA traces were then used to determine heat-treatment schedules for forming glass-ceramics.

Temperature ranges for nucleation and crystal growth determined from the DTA and the DSC data were employed in the heat-treatment processes. Glasses were heat treated by heating at 5 K min^{-1} to the exothermic peaks indicated on the DTA curves, holding for 1 h, and then quenching in air.

Powder diffraction patterns were obtained using a Phillips Diffractometer model 12045 utilizing CuK_α radiation. Samples of as-quenched glasses, heat-treated glasses and commercial samples (supplied by Corning Inc.) were ground to ca. 320 mesh and were investigated on a zero-background holder. Scans ranged from 2θ positions of 10–60 °C with a step size

of 0.02° and a count time of 1 s. The spectra were analysed using Siemens D500 software.

Nucleation characterization of samples was carried out by transmission electron microscopy (TEM) with an accelerating voltage of 200 kV. Nucleated samples were prepared from annealed glasses which were sliced to a thickness of ca. 2 mm and cut into 1–2 mm disks, then heated in a DTA unit at a heating rate of 5 K min^{-1} to the selected nucleating temperature. Devitrified samples were thinned to ca. 100 μm, dimpled and milled by ion-milling. The presence of crystalline phases was confirmed by dark-field analysis.

Scanning electron microscopy (SEM) was used to observe crystal morphology on fracture surfaces and polished samples (etched with 2% HF) of glass-ceramics prepared in the laboratory and a commercial canasite glass-ceramic (Corning Glass Works, Corning, NY).

3. Results and discussion

F analysis of the four glasses presented in Table II indicate a decrease in F by ca. ≈ 15–30 wt % of the original value. Previous work [7, 8] indicates that the loss is primarily due to volatilization of F as SiF_4 and NaF during melting. Increased melting time, or use of an uncovered crucible, greatly increased the loss and strongly influenced the resulting glass properties. The densities of the glasses differed only slightly, all being ca. 2.6 g cm^{-3}. T_g of glasses 1–4, determined from DSC curves in Fig. 1a–d, respectively, decreased as the wt % F in the glasses increased. This is consistent with previous observations [8]. Substitution of CaF_2 for the number of Si–O–Si linkages (replaced by two Si–F bonds) resulted in weakening of the overall glass network structure, and is reflected in decreased T_g of glasses and decreased viscosities of the melts [7, 8].

The glasses melted from compositions 1–3 were clear, while that from composition 4 was white and semi-opaque. The opalization in glass 4 resulted from the precipitation of CaF_2 crystals during glass formation. The existence of CaF_2 crystals was confirmed by the XRD pattern seen in Fig. 2. The peak patterns absolutely matched the standard pattern JCPDS #35-618 for CaF_2 (fluorite).

The DTA curves of glasses 1–4 in Fig. 3a–d, respectively, show two distinct exothermic peaks for glasses 1–3, while that of glass 4 exhibits three exothermic peaks. Temperatures corresponding to these peaks, shown in Table III, can be assigned to the crystallization of various phases. The crystalline phases corresponding to each exothermic peak were identified by XRD. XRD patterns of glass 1 heated at 640 and 717 °C, the first and second exotherms, respectively, as seen in Figs 4a and 5a, respectively, show broad spectra representing an amorphous structure. The specimens were clear after being heated at 640 °C, but were deformed and translucent after being heated at 717 °C. No further attempts were made to crystallize this glass.

XRD patterns of glasses 2 and 3, which were heat treated at 630 and 580 °C, respectively, the first exotherm for both glasses, are shown in Fig. 4b and c, respectively. Both glasses exhibited a foggy appearance. The presence of a crystal phase which matched the standard pattern for CaF_2 (JCPDS #35-618) is confirmed in both cases.

XRD patterns of glasses 2 and 3 which were heat treated at 740 °C, and the second exothermic peak temperature, are shown in Fig. 5b and c, respectively. The two crystallized glasses were white and semi-opaque. The pattern most closely matched the JCPDS #13-553, i.e. canasite. They also matched XRD patterns of a commercial canasite glass-ceramics.

TABLE I Glass composition in mol %

Composition no.	SiO_2	CaO	CaF_2	Na_2O	K_2O	Al_2O_3
1	60.8	14.6	8.6	9.3	5.4	1.3
2	60.8	12.6	10.6	9.3	5.4	1.3
3	60.8	8.6	14.6	9.3	5.4	1.3
4	60.8	4.6	18.6	9.3	5.4	1.3

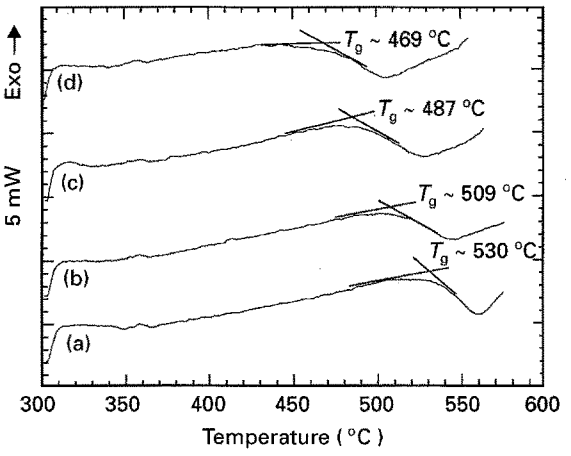

Figure 1 The DSC curve of glasses: (a) 1; (b) 2; (c) 3; and (d) 4.

TABLE II Characteristics of glass compositions

Composition no.	Fluorine of original composition (wt %)	Fluorine of as-quenched glass (wt %)	T_g (°C)	Density (g cm^{-3})
1	5.2	3.6	530	2.607
2	6.3	5.2	509	2.606
3	8.6	6.7	487	2.602
4	10.8	8.8	469	2.573

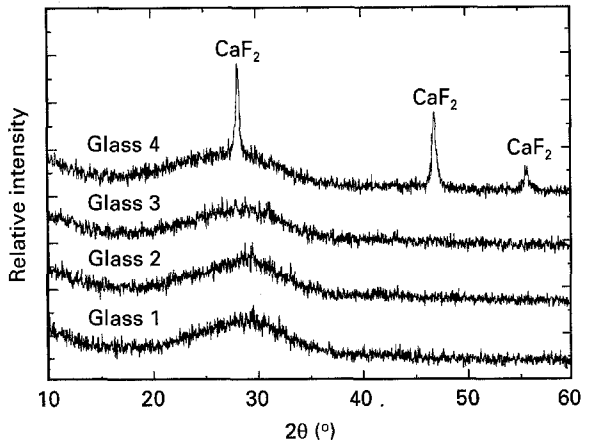

Figure 2 The XRD pattern of as-quenched glasses 1–4.

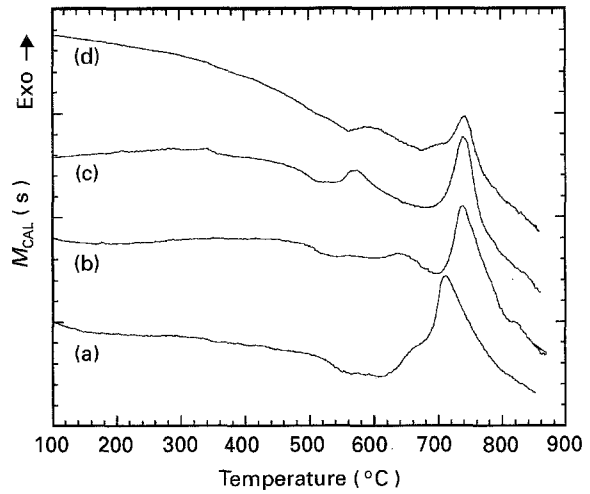

Figure 3 The DTA curve of glasses: (a) 1; (b) 2; (c) 3; and (d) 4.

TABLE III Exothermic peak temperature of glass compositions on the DTA curves

Composition no.	First exotherm (°C)	Second exotherm (°C)	Third exotherm (°C)
1	640	717	–
2	630	740	–
3	580	740	–
4	580	700	745

The two samples of glass 4, one heat treated at 580 and the other at 700 °C, the first and second exotherms, respectively, are shown in Fig. 4d and c, respectively. The crystallized glasses after heating at 580 and 700 °C were white and semi-opaque. They have identical XRD patterns with CaF_2 as the crystalline phase. After heating at 745 °C, the third exotherm, the crystallized glass became more opaque but the sample cracked and the evidence of surface crystallization was seen. The XRD pattern in Fig. 5d shows neither peak positions nor relative peak intensities corresponding to canasite or to those of the commercial sample. The dominant phase present in glass 4 after heating at 745 °C is CaF_2, together with agrellite (JCPDS #29-1188).

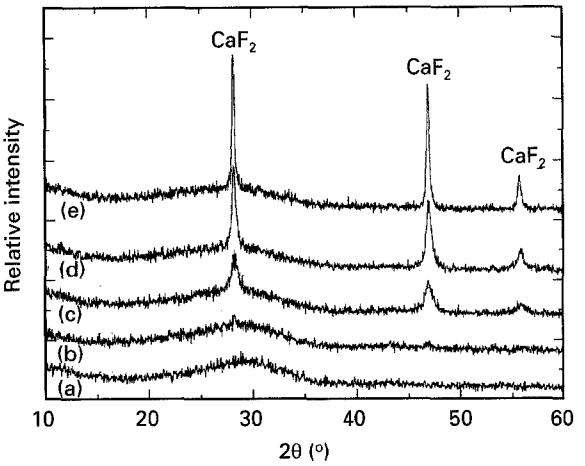

Figure 4 The XRD patterns of glasses 1–4, heated at the temperature corresponding to the first exothermic peak: (a) glass 1 at 640 °C; (b) glass 2 at 630 °C; (c) glass 3 at 580 °C; (d) glass 4 at 580 °C; and (e) glass 4 at 700 °C.

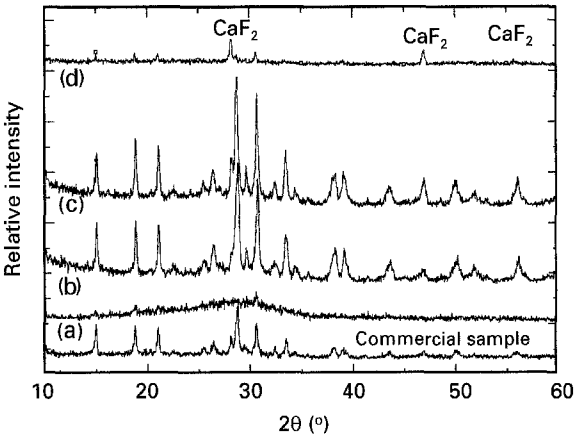

Figure 5 The XRD patterns of glasses 1–4 heated at the temperature corresponding to the second exothermic peak: (a) glass 1 at 717 °C; (b) glass 2 at 740 °C; (c) glass 3 at 740 °C; and (d) glass 4 at 745 °C. Cf. with the commercial canasite sample.

The TEM micrographs of glass 2, devitrified at 630 °C, show fairly large and non-uniformly distributed nuclei. The spherical nuclei with a mean size of ca. 250 nm are obvious, Fig. 6a. Smaller and more uniformly dispersed nuclei can be observed in the TEM micrographs of glass 3, devitrified at 580 °C, shown in Fig. 6b. Nuclei obtained from glass 3 had a mean particle diameter of 20 nm.

EDS was performed on the samples during the TEM investigation in order to distinguish chemical elements in the matrix region from chemical elements in the nuclei. In heat treated glass 2, in which the nuclei and the matrix were distinguishable, the result shows that the nuclei had a greater concentration of Ca and F than the matrix. The intensity of F at these two sites is not obviously different, owing to the loss of F via volatilization caused by the electron beam during the investigations. These results are in agreement with the previous identification of CaF_2 by XRD, as shown previously in Fig. 5.

EDS was also done on heat treated glass 3, which had high concentrations of tiny nuclei. Since the nuclei

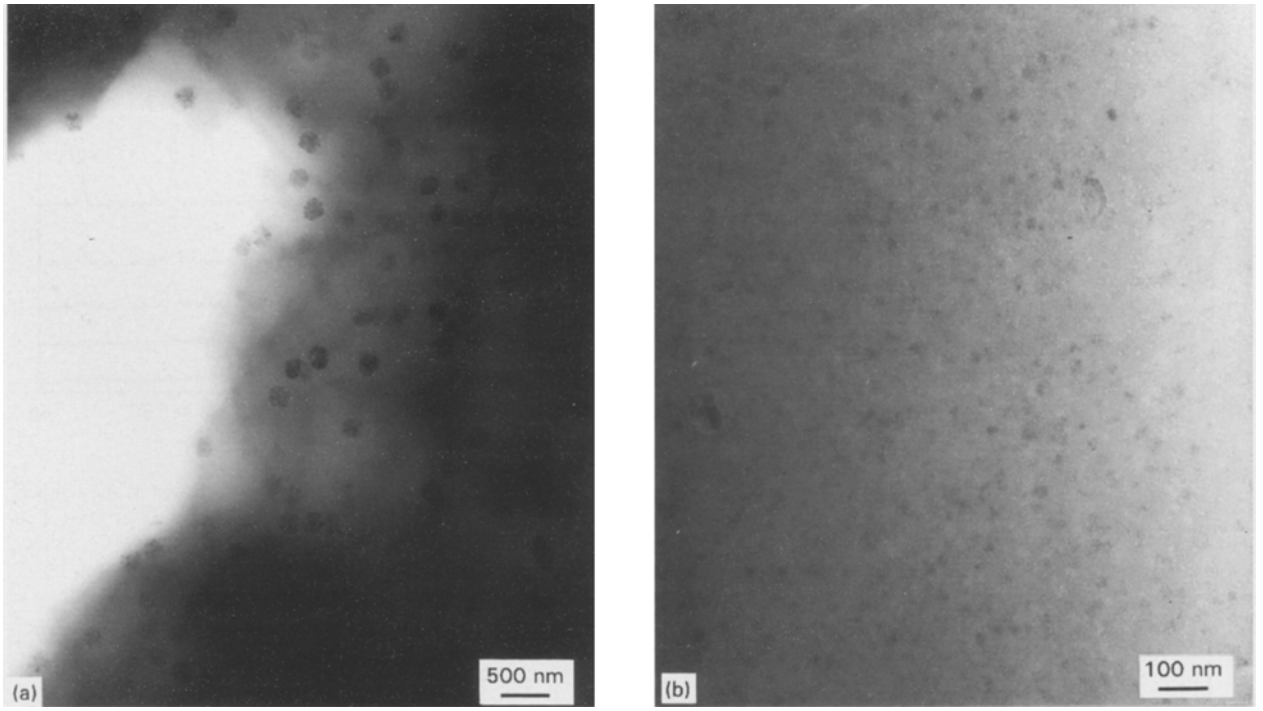

Figure 6 TEM micrographs of: (a) glass 2 heated at 630 °C and (b) glass 3 heated at 580 °C.

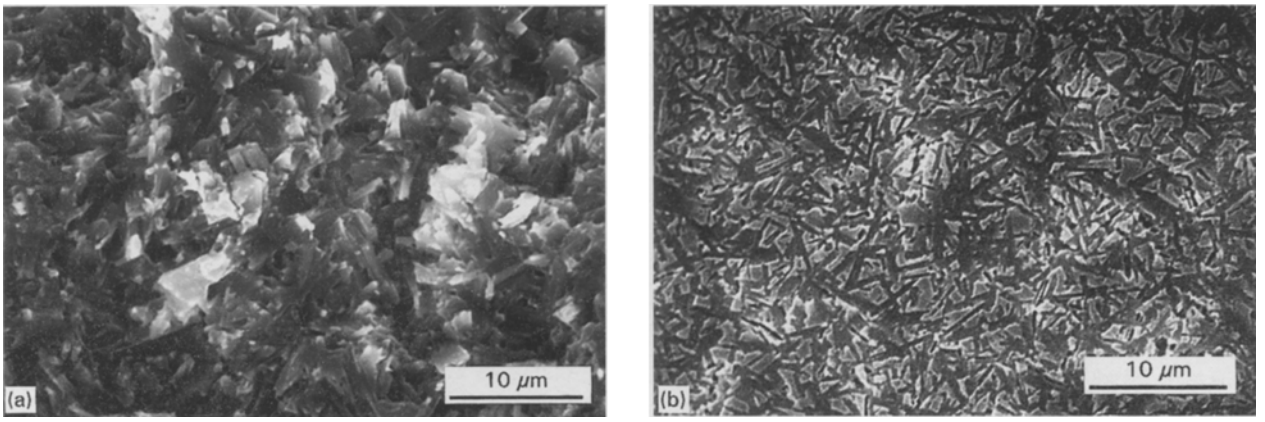

Figure 7 SEM micrographs of: (a) fracture surface on commercial sample and (b) polished and etched commercial sample.

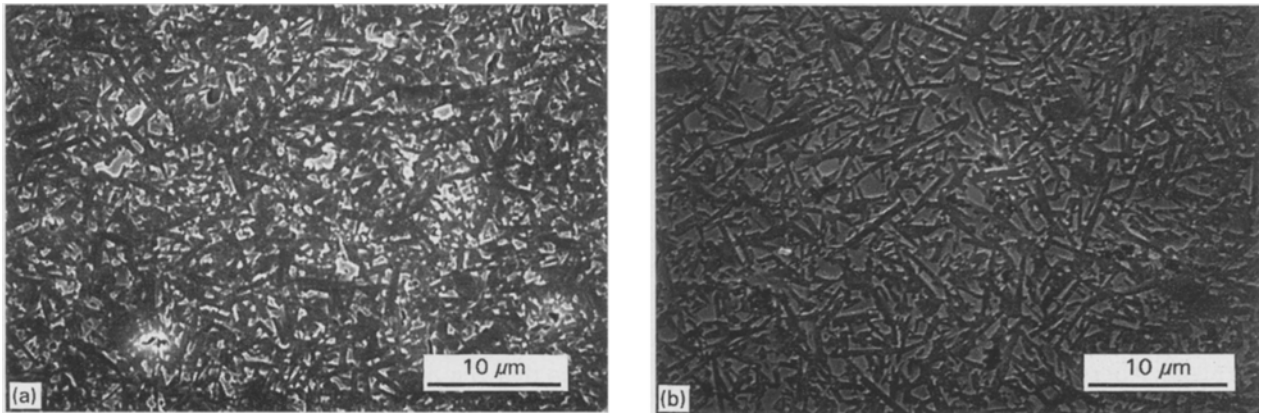

Figure 8 SEM micrographs of polished and etched samples: (a) glass 2 and (b) glass 3.

were much smaller than the electron beam, it was difficult to distinguish individual nuclei from the matrix. Therefore, the spectrum shows a mixture of chemical elements present in the matrix and in the nuclei. This prevents us from distinguishing the chemical elements present in the nuclei.

The TEM micrographs confirm the presence of nuclei achieved from the heat treatment processes; the

existence of CaF_2 nuclei were disclosed by the XRD. The number and size of nuclei correlated directly with the F content in the parent glasses.

Microstructure on fracture surfaces of crystallized glasses 2, 3 and commercial canasite glass-ceramics show interlocking blades and effects of cleavage splintering, as seen in Fig. 7a.

On the etched specimens, highly interlocking blade-like grains, shown in Figs. 7b, 8a and b, are clearly seen in every specimen. The increase in the amount of blade-like grains in crystallized glass 3, owing to the higher F content in the parent glasses, is obvious when a comparison is made with crystallized glass 2 which contained less F.

4. Conclusions

Present results indicate that the F content of the parent glass is critical for the formation of canasite glass-ceramics. F is required for both nucleation by CaF_2 and, since it is a constituent of canasite, it must also be available during the crystallization step. Too low an F content resulted in a deficiency of F for nuclei formation and inhibited the formation of canasite crystals. Too high an F concentration resulted in precipitation of CaF_2 in the as-quenched glass. The growth of these pre-existing CaF_2 crystals accompanied by the formation of additional CaF_2 crystals due to heat treatment evidently depleted the remaining F in the glass phase and competed with canasite crystal formation, and allowed the formation of an agrellite crystalline phase.

Acknowledgement

We wish to thank Drs C. Leonelli and S. Bigi, Institute of Mineralogy and Petrology, Modena University, Italy, for analysing the K_α radiation of F atoms.

References

1. G. H. BEALL, *Solid State Sci.* **3** (1989) 333.
2. *Idem. Corning Research* (Corning Annual Report) (1973) 99.
3. D. G. GROSSMAN, in "Advances in ceramics", edited by J. H. Simmons, D. R. Uhlmann and G. H. Beall (The American Ceramic Society, Columbus, Ohio, 1982) p. 249.
4. G. H. BEALL, *J. Non-Cryst. Solids* **129** (1991) 163.
5. *Idem.* US Patent 4 386 162 (May 31, 1983).
6. *Idem.* US Patent 4 397 670 (August 9, 1983).
7. P. W. MCMILLAN, "Glass ceramics" 2nd edn (Academic Press, New York, 1979) p. 84.
8. Q. A. JUMA'A and J. M. PARKER, in "Advances in Ceramics", edited by J. H. Simmons, D. R. Uhlmann and G. H. Beall (The American Ceramic Society, Columbus, Ohio, 1982) p. 218.

Received 6 March
and accepted 24 May 1995